ON THE FORMATION OF THE HEMISPHERIC DICHOTOMY OF ENCELADUS. L. Han[1] and A.P. Showman[2], [1]Planetary Science Institute, 1700 E Fort Lowell, Suite 106, Tucson, AZ 85719. han@psi.edu, [2] Department of Planetary Sciences, Lunar and Planetary Laboratory, University of Arizona, Tucson, AZ 85721.

Introduction: Saturn's moon Enceladus has enjoyed a rich tectonic history. Its surface exhibits a diversity of tectonized terrains, including ridges, grooves, grabens, and rifts that cover a significan fraction of the surface [1-2]. Particularly striking is the south polar terrain (SPT), which includes the "tiger stripes," ∼130-km-long fractures exhibiting high temperatures [3-4] and jetting salty ice particles and various gases into space [5-7]. Few craters exist in the SPT, suggesting ages of 10–100 Myr or less. In contrast, the terrains in the northern hemisphere are heavily cratered, relatively ancient, and show no signs of current activity.

This hemispheric dichotomy of tectonism and heat flu has proved difficul to explain. Several authors have suggested that convection [8-11] or a local ocean [12-13] coupled with local tidal dissipation may allow the activity at the SPT. However, previous 3D spherical models of thermal convection in Enceladus' ice shell have failed to explain the dichotomy between the northern and southern hemispheres. Here we present new 3D models that demonstrate (1) how localized active regions can result from brittle deformation, and (2) how appropriate topography on the silicate core can modulate the convection in the ice-shell and allow activity to be preferentially focused in one hemisphere.

Model and Methods: Adopting the Boussinesq approximation and infinit Prandtl number, the momentum, continuity, and energy equations governing convection in Enceladus' ice shell are

$$\nabla\sigma + RaT\overrightarrow{r} = 0 \tag{1}$$

$$\nabla \cdot v = 0 \tag{2}$$

$$\frac{\partial T}{\partial t} + v \cdot \nabla T = \nabla^2 T + q \tag{3}$$

where σ is the stress tensor, T is temperature, Ra is the Rayleigh number, v is the 3D velocity, $\overrightarrow{r}$ is the radial (outward) unit vector, t is time, and q is the tidal heating. All variables are non-dimensional. We solve these equations in a 3D spherical shell using the finite-elemen code CitcomS [14].

We adopt a Newtonian, temperature-dependent viscosity appropriate for ice:

$$\eta = \eta_0 \exp\left[A\left(\frac{1}{T} - 1\right)\right] \tag{4}$$

where η_0 is the reference viscosity at the base of the ice shell and $A = 26$, corresponding to an activation energy of 60 kJ mol^{-1}. We apply a cutoff that prevents the viscosity from rising above $\Delta\eta$ times η_0, where $\Delta\eta$ is the viscosity contrast. Most of our runs adopt $\Delta\eta = 10^5 - 10^8$, ensuring that the convection will occur in the stagnant-lid regime in the absence of brittle deformation (see below).

To investigate the effects of brittle deformation, we include plastic rheology. Plastic deformation occurs only when

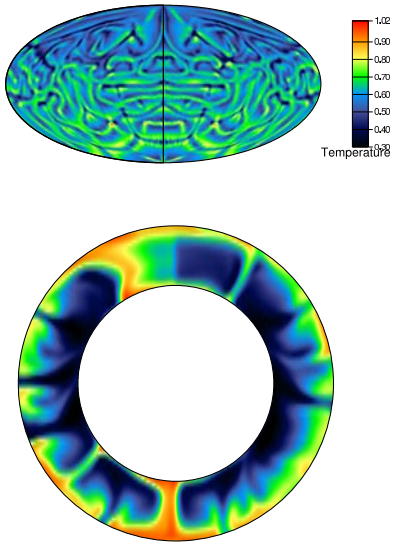

Figure 1: Temperature structure from a full 3D spherical model showing thermal convection in Enceladus' ice shell during a lithospheric overturn event. The simulation adopts a Rayleigh number of 5×10^7, a viscosity contrast $\Delta\eta = 10^5$, and a yield stress of 0.5 bar. The top panel displays the temperature distribution on a constant radius spherical surface at depth of 66 km. The bottom panel displays temperature distribution along the radial cross-section shown by the solid line in the top panel. In the simulation, a stagnant lid builds, then undergoes a global overturn (shown), after which the stagnant lid regrows, and the cycle repeats episodically. In absence of core topography, the overturns are usually global as shown here.

deviatoric stresses reach a specifi yield stress σ_Y. Following previous work [15-17,10], the plasticity is incorporated by means of an effective viscosity

$$\eta_{eff} = \min\left[\eta(T), \frac{\sigma_Y(z)}{2\dot{\epsilon}}\right] \tag{5}$$

where $\eta(T)$ is the thermally activiated creep viscosity given by Eq. 4 and $\dot{\epsilon}$ is the second-invariant of the strain-rate tensor.

We adopt an ice-shell thickness of 100 km, consistent with estimates for a differentiated interior. The surface temperature is maintained at 70 K, while the basal temperature is fi ed at 260-270 K. The top mechanical boundary conditions is free-slip, while the bottom boundary condition is no-slip.

In some models, we explore the effect of topography at the top of the silicate core. As noted by McKinnon [18], asteroids similar in size to Enceladus exhibit significan topography, and under conditions relevant to Enceladus, the silicate core can maintain topography indefinitel . Suppose the topography

measured relative to the bottom of the domain is $h(\lambda, \phi)$, where λ is longitude and ϕ is latitude. To represent the effect of core topography, we introduce a viscosity contrast of 10^{10} for all regions at and below a height $h(\lambda, \phi)$, thereby limiting ice fl w to regions outside of that surface.

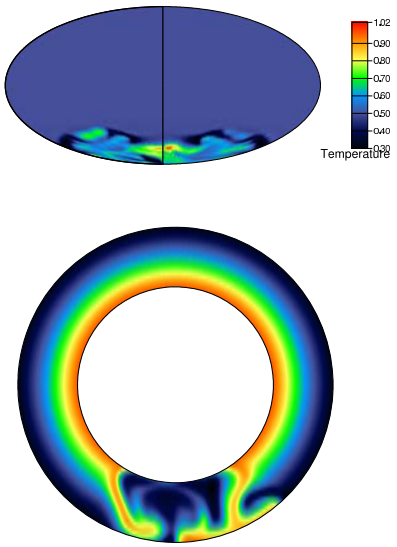

Figure 2: Temperature profil from a full 3D spherical model, including core topography, showing the confinemen of an overturning event to the south polar region. The simulation adopts a Rayleigh number of 7×10^7, a viscosity contrast $\Delta\eta = 10^5$, and a yield stress of 0.5 bar. The top panel displays the temperature distribution on a constant radius spherical surface at depth of 66 km. The bottom panel displays temperature distribution along the radial cross-section shown by the solid line in the top panel. The overturns occur episodically, as in Figure 1, but here they occur only southward of $\sim70^\circ$S latitude.

Results: We firs consider cases with no core topography. When the yield stress is large ($\sigma_Y \geq 1$ bar), the convection occurs under a thick stagnant lid, if at all; the heat flu is small ($\sim$5–10 mW m^{-2}) and there is no hemispheric dichotomy in the convection. When the yield stress is small, however, plastic deformation can occur, forcing the convection away from the stagnant-lid regime. Moresi and Solomatov [15] identifie two regimes. At low yield stresses, the convection enters a mobile-lid regime, where the plasticity allows continual overturning of the lithosphere. At higher yield stresses, the overturning is episodic: the stagnant-lid thickness builds until stresses reach the yield stress, whereupon plastic deformation causes the lid to overturn and allows warm, mobile ice to reach close to the surface. O'Neill and Nimmo [10] argued that, if such episodic overturn events were regionally confined they could explain the regional nature of the tectonic terrains on Enceladus. However, our 3D models show that, at realistic viscosity contrasts, episodic overturning events, even if locally initiated, tend to expand into full global overturns. Figure 1 illustrates an example. A stagnant lid forms, becomes unstable, overturns (shown), and then a new stagnant lid grows and the cycle repeats episodically. This class of behavior, by itself, therefore fails to explain the regional confinemen of Enceladus' current activity to the South Polar Terrains.

We next explore cases with core topography. We fin that appropriate global-wavenumber-one topography, with the ice shell slightly thicker at the south pole than elsewhere, can allow convection to occur preferentially at the south pole. Figure 2 illustrates an example with topography of 10 km and a yield stress $\sigma_Y = 0.5$ bar. The convection is mobile-lid and, importantly, is confine to regions near the south pole. The stagnant lid grows, becomes locally unstable, and overturns—*but only regionally near the south pole*. After the regional overturn the stagnant lid regrows in the affected area and the cycle repeats. No convection, and no overturning, occurs in Enceladus' northern hemisphere, consistent with the ancient ages of most of the terrains there. This model can naturally explain the confinemen of Enceladus' activity to the SPT.

Our model can also explain the apparent contradiction between the current massive heat flu and the limited total power budget available to Enceladus. In our models, the heat flu es at the SPT during the overturn (Fig. 2) reach $\sim$100–200 mW m^{-2}, in agreement with the observed heat flux Nevertheless, because the overturn events typically occur during only $\sim$1% of the total history, the *time-mean* heat flu is relatively low. Thus, our models help to resolve the conundrum that, for realistic orbital histories, the available tidal heating on Enceladus is too small to maintain the observed heat flu in steady state [19].

Conclusions and Discussions: Our models show that topography on the core of Enceladus may play a key role in affecting the convective regime and confinin the current active tectonics and high heat flu to the southern hemisphere.

Ackhnowledgement: This work is supported by NASA OPR Program.

References: **[1].** Kargel, J.S., and S. Pozio (1996) Icarus 119, 385-404. **[2].** Porco, C.C., et al. (2006) Science 311, 1393-1401. **[3].** Spencer, J.R., et al. (2006) Science 311, 1401-1405. **[4].** Howett, C.J.S., et al. (2011) JGR, doi:10.1029/2010JE003718. **[5].** Hansen, C.J., et al. (2006) Science, 311, 1422-1425. **[6].** Brown, R., et al. (2006) Science, 311, 1425-1428. **[7].** Postberg, F., et al. (2009). Nature 459, doi:10.1038/nature08046. **[8].** Barr, A.C. (2008) JGR 113, doi:10.1029/2008JE003114. **[9].** Roberts, J.H., and F. Nimmo (2008) GRL 35, doi:10.1029/2008GL033725. **[10].** O'Neill, C., and F. Nimmo (2010) Nature Geoscience, doi:10.1038/NGEO731. **[11].** Han, L., et al. (2012) Icarus, doi:10.1016/icarus.2011.12.006. **[12].** Collins, G.C., and J.C. Goodman (2007) Icarus 189, 72-82. **[13].** Tobie, G., et al. (2008) Icarus doi:10.1016/ j.icarus.2008.03.008. **[14].** Zhong, S.J., et al. (2000) JGR 105, 11063-11082. **[15].** Moresi, L., and V. Solomatov (1998) Geophys. J. Int. 133, 669-682. **[16].** Tackley, P.J. (2000) Science 288, 2002-2007. **[17].** Showman, A.P., and L. Han (2005) Icarus 177, 425-437. **[18].** McKinnon, W.B. (2011), Enceladus workshop abstract. **[19].** Meyer, J., and J. Wisdom (2007) Icarus 188, 535-539.